27
1-29-81
2 to NTIS

①

R-1496

MASTER

UCID- 18979

Sausage Mode Stability Boundaries - Enumeration and Verification

Frank W. Chambers

December 2, 1980

Lawrence Livermore Laboratory

Sausage Mode Stability Boundaries – Enumeration and Verification*

Frank W. Chambers

December 2, 1980

Abstract

An axially symmetric sausage mode instability has been observed using particle simulation codes to propagate beams with a high degree of current neutralization. In this report the stability boundaries in terms of the magnitude and location of the return current are delineated for beams with square, Gaussian, and Bennett radial current profiles using the theoretical analysis of others. For the case in which the return current is held fixed as the beam propagates, a detailed comparison is made between the theoretical predictions and the results of the RINGFAST single disk particle simulation code. Agreement between theory and code results is good although the code results do show a slightly larger than predicted unstable region.

*Lawrence Livermore National Laboratory is operated by the University of California for the Department of Energy under Contract W-7405-ENG-48.

This work was performed by LLNL for the Department of Defense under DARPA (DOD) ARPA Order 3178, Amendment No. 12, monitored by NSWC under Contract No. N60921-80-WR-W0188.

Introduction

Computer calculations of electron beam propagation in gas using the RINGBEARER particle simulation code[1,2] have exhibited a sausage mode instability[3] in beam and gas parameter regimes where there is a high degree of current neutralization. Theoretical predictions of the threshold, growth rate, and pulse response for a sausage unstable beam have recently been published[4,5]. In this report results for the sausage mode dispersion relation and stability boundaries from reference 4 are summarized. Numerical plots of stability boundaries for square, Gaussian, and Bennett beams are given. The sausaging of a beam segment with a fixed return current is studied using the RINGFAST single disk simulation code[3]. The observed thresholds and growth rates for Gaussian and Bennett beams are compared with theoretical predictions.

Summary of Analytic Results from Reference 4

The sausage mode analysis[4] is performed for a beam propagating in the positive Z direction; Z being the distance of a beam segment from the point of injection. The coordinate X gives the distance of the beam segment from the beam head. The spatial and temporal variation of the mode is assumed to have the form:

$$\exp(-i\Omega\bar{k}Z+pX/\lambda_m) \qquad (1)$$

Here $\bar{k}$ is the averaged betatron wavenumber to be discussed later. The parameter λ_m is the magnetic decay length; $\lambda_m = 4\pi\sigma R^2/c$, σ being the on-axis conductivity, R the beam root mean square radius, and c the velocity of light. The mode wavenumbers Ω and p are dimensionless.

The dispersion relation describing the sausaging of a beam in the presence of a return current is:

$$D(\Omega,p) = (\Omega^2+i\alpha\Omega-S)\ (p+1) + T \tag{2}$$

where:

$$S = (2\Gamma+A-ABf_m)/\Gamma \tag{3}$$

$$T = A/\Gamma \tag{4}$$

and:

$$A = \int dr\ 8\pi^2 r^3\ \left(\frac{J_B}{I_B}\right)^2 \tag{5}$$

$$B = \frac{1}{A} \int dr\ 8\pi^2 r^3\ \left(\frac{J_B}{I_B}\frac{J_P}{I_P}\right) \tag{6}$$

$$\Gamma = 1-(2-C)f_m \tag{7}$$

$$C = 2\int dr\ \left(\frac{I_{BR}}{I_B}\right)\left(\frac{2\pi r J_P}{I_P}\right) \tag{8}$$

$$f_m = I_P/I_B \tag{9}$$

$$I_{BR} = \int_0^r 2\pi r dr\ J_B \tag{10}$$

Here J_B and J_P are the beam and return current density profiles, I_B and I_P are the total beam and plasma currents (I_P is assumed to be directed opposite to I_B). The quantity f_m is the fractional current neutralization, Γ measures the reduction in the effective pinch potential due to the presence of the return current. If $f_m = 0.0$, then $\Gamma = 1.0$. The parameter α characterizes the phase mix damping of the betatron oscillations[5]. A, B, and C describe the beam and return current profiles. The parameters A, B, and C are given in Table I for a square profile, a Gaussian profile, and a Bennett profile. In each case the return current profile is assumed to be identical to that of the beam but with a different characteristic radius. For the case where the beam and plasma have identical profiles with identical radii $B = C = 1.0$ and $\Gamma = 1-f_m$.

TABLE I

PROFILE PARAMETERS A, B, AND C

$$\eta^2 = R_P^2/R_B^2$$

Square beam, Square return current:

$$J_B = \frac{I_B}{\pi R_B^2} \quad r<R_B \qquad\qquad J_P = \frac{I_P}{\pi R_P^2} \quad r<R_P$$

$$= 0 \quad r>R_B \qquad\qquad = 0 \quad r>R_P$$

$$A = 2.0$$

$$B = \eta^2 \qquad \eta^2<1.0$$

$$1/\eta^2 \qquad \eta^2>1.0$$

$$C = \eta^2 \qquad \eta^2<1.0$$

$$2-1/\eta^2 \qquad \eta^2>1.0$$

Gaussian beam, Gaussian return current:

$$J_B = \frac{I_B}{\pi R_B^2} \exp(-\frac{R^2}{R_B^2}) \qquad\qquad J_P = \frac{I_P}{\pi R_P^2} \exp(-\frac{R^2}{R_P^2})$$

$$A = 1.0$$

$$B = \frac{4\eta^2}{(1+\eta^2)^2}$$

$$C = \frac{2\eta^2}{1+\eta^2}$$

Bennett beam, Bennett return current:

$$J_B = \frac{I_B/\pi R_B^2}{(1+R^2/R_B^2)^2} \qquad\qquad J_P = \frac{I_P/\pi R_P^2}{(1+R^2/R_P^2)^2}$$

$$A = 2/3$$

$$B = \frac{\eta^2}{A}(\frac{-6}{(\eta^2-1)^2} - \frac{4(\eta^2+1)}{(\eta^2-1)^3} \ln(1/\eta^2))$$

$$C = 2 - \frac{2}{(\eta^2-1)^2} (1.0-\eta^2+\eta^2 \ln(\eta^2))$$

Stability Boundaries

Several boundaries in f_m and η^2 exist for the beam and are plotted in figures 1,2, and 3. For a pinch to exist at all one must have:

$$\Gamma > 0 \tag{11}$$

The threshold for instability with either p = 0.0 or $\Omega = 0.0$ is:

$$(S-T) < 0 \tag{12}$$

Equation 12 does not represent an absolute instability criterion. An observer in the beam frame (X fixed, $Z \to \infty$) will see a perturbation decay as $\exp(-(\alpha/2)\bar{k}Z)$. An observer in the lab frame (Z fixed, $X \to \infty$) will see a perturbation decay as $\exp(-X/\lambda_m)$. There is no absolute instability in either the beam or the laboratory frame. The $\Omega = 0$ and $p = 0$ cases correspond to specific initial conditions in X and Z. A mode with $\Omega = 0$ would be excited by a perturbation placed at a specific X and held fixed for all Z. The dispersion relation with $\Omega = 0$ will then describe the evolution in X of the beam behind this perturbation. Such an initial condition might be set up by the beam neck down region which represents a perturbation nearly fixed in X. The $p = 0$ instability will be excited by a perturbation which is uniform in X. Since the beam has a head and a tail no such excitation is possible except in an approximate sense as discussed later. However, the $p = 0$ instability can be studied using a single disk simulation code and hence is useful for understanding and verifying the sausage mode analysis.

The condition for convective instability is that $Re(p_{max}) > 0.0$ where p has been maximized over $Re(\Omega)$ with $Im(\Omega) = 0$. In terms of S and T this boundary is:

$$\frac{T+\alpha^2}{2\alpha S^{1/2}} < 1 \tag{13}$$

The growing perturbation will be convecting at a velocity which is greater than zero but less than the beam velocity[7].

These boundaries are indicated in figures 1,2, and 3 for the cases with a square beam with a square return current, Gaussian beam with a Gaussian return current, and for a Bennett beam with a Bennett return current as described in Table I. Several features emerge from figures 1,2, and 3. The square beam shows the highest degree of instability and is convectively unstable even in the absence of a return current. As $R_P \to 0$ in all cases one finds no pinch if $f_m > .5$. When $R_P = R_B$ one finds, as expected, there is no pinch if $f_m > 1.0$. Looking at the boundary for forming a stable pinch one finds that below $\eta^2 \approx 1.0$ the Bennett beam allows the largest f_m and the square beam the lowest f_m for a fixed η^2. Above $\eta^2 = 1.0$ the situation is reversed and the square beam is the easiest to pinch, the Bennett is the most difficult. Considering the $p = 0$ or $\Omega = 0$ instability in each case with $\eta^2 = 0.0$ the boundary is at $f_m = .5$. At $\eta^2 = 1.0$ the thershold for instability for the square beam is $f_m = .5$, for the Gaussian $f_m = .667$, and for the Bennett $f_m = .75$. The square beam exhibits the largest convectively unstable regime, the Gaussian beam shows a smaller unstable region, and the Bennett beam has the smallest region. Figures 1,2, and 3, graphically exhibit the need to consider realistic beam profiles when computing sausage mode stability. Physically, the origin of this decreasing susceptability to sausaging is the increased width of the betatron frequency spectrum as one moves to more rounded beam radial profiles.

p = 0 Instability

The case where p = 0.0 corresponds to the sausaging of a beam uniform in X with no variation in $J_p(R)$ as the beam evolves in Z. In an actual beam $J_p(r)$ will vary in X and will decay in X on a distance scale $\lambda_{m0} \sim \pi\sigma R^2/c \ \ln(b/R)$ where b is the maximum radius to which significant conductivity is generated. Local perturbations in the plasma current decay on the more rapid length scale. $\lambda_m \sim 4\pi\sigma R^2/c$. For a beam segment with $\lambda_m < X < \lambda_{m0}$ the sausage mode will be described by the above dispersion relation with p = 0 at least for a brief propagation distance. This aspect of the instability can be studied using a single disk simulation code such as the RINGFAST code[3].

The RINGFAST code has been modified to allow the loading of particles in velocity equilibrium[8] for several beam and return current profiles. Runs were made with $R_B = R_p$ ($\eta^2 = 1.0$) to determine the stability and growth rates for sausage mode. The theoretical growth rate with p = 0.0 is given by:

$$\Omega = \frac{-\alpha}{2} + (S - T - \frac{\alpha^2}{4})^{1/2} \qquad (14)$$

The threshold for instability is T>S. The term Ω is normalized to $\bar{k}$ where $\bar{k}$ is $(\overline{k_\beta{}^2 r^2})^{1/2}/R$. When the beam and return currents have the same profiles $\Gamma = (1-f_m)$, $\overline{k_\beta{}^2 r^2} = ((1-f_m)(I_B/I_A))$, and I_A is the Alfven current, $I_A = 17050\ \gamma$ Amps. Here γ is the usual Lorentz factor characterizing the beam energy. Thus in units of cm^{-1}:

$$\Omega(\mathrm{cm}^{-1}) = \Omega((1-f_m)(\frac{I_B}{I_A}))^{1/2}/R \qquad (15)$$

Square Beam, Square Return Current

The predicted growth rate for the p = 0 instability for a square beam with a square return current of equal radius ($R_p = R_B$, $\eta^2 = 1.0$) is obtained from equation 14 with $\alpha = 0.0$. One finds:

$$\Omega^2 = (\frac{2(1-2f_m)}{1-f_m}) \qquad (16)$$

The beam is unstable if $f_m > .5$. The growth rate in inverse centimeters for $f_m > .5$ is:

$$\mathrm{Im}(\Omega)(\mathrm{cm}^{-1}) = 2^{1/2}(\frac{I_B}{I_A})^{1/2} \frac{(2f_m-1)^{1/2}}{R} \qquad (17)$$

For the square beam, $I_B/I_A = \omega_{pB}{}^2R^2/4$ where $\omega_{pB}{}^2 = 4\pi n_B e^2/\gamma m_e$. Here n_B is the beam particle density, $n_B = I_B/(\pi R_B{}^2 ec)$, and e and m_e are the charge and mass of the electron. Substituting in equation 17, recalling $R = R_r/2^{1/2}$, gives:

$$\mathrm{Im}(\Omega) = \frac{\omega_{pB}}{c} (2f_m-1)^{1/2} \qquad (18)$$

This result is identical to that obtained in reference 5 for the square beam case in this limit.

Gaussian Beam, Gaussian Return Current

RINGFAST was run for a Gaussian beam with parameters given in Table II. For these runs the beam, when unstable, collapsed inward to a smaller radius. The e-folding distance for the perturbed root mean square radius is determined from semilog plots. The collapse halts at the radius R_{min} specified in Table II. When R_{min} > .85 cm the beam did not collapse to any great extent and the tabulated growth rates have a high degree of uncertainty. The results are collected in figure 4 along with the theoretical predictions from equations 14,15. The simulation exhibited instability for lower f_m than predicted although growth rates below Ω_i = .01 are not reliable since the beam radius may simply be adjusting to an imperfect match at injection. At f_m = .5 for the Gaussian case a run was made with the return current radius reduced to R_p = .99 so the beam would expand instead of collapsing. This run was found to be stable. The minimum f_m for instability is significantly less than the predicted value of f_m = .667.

TABLE II

RINGFAST RUNS, GAUSSIAN BEAM, GAUSSIAN RETURN CURRENT

I_B = 10000.0 A
γ = 100
R_B = 1.0 cm
R_p = 1.0 cm

f_m varied by varying I_p

f_m	λ_{efold} cm	R_{min} cm	Ω_i cm^{-1}
.90	16.4	.456	.061
.85	19.5	.489	.051
.80	21.1	.532	.047
.75	26.6	.615	.038
.70	28.3	.742	.035
.65	28.4	.846	.035
.60	42.0	.890	.024
.50	135.	.945	.007
.50	270.	.912	.004
.45	255.	.928	.004
.50*	----	.960	----
.75*	19.9	----	.050

* These runs were made with R_p reset to .99 causing the beam to expand instead of collapsing when the beam is unstable.

Bennett Beam, Bennett Return Current

For the Bennett beam with a Bennett return current the RINGFAST results and theoretical prediction are shown in figure 5. Beam and code parameters are given in Table III. For these runs f_m was varied by varying I_B and I_P while maintaining $I_B - I_P = 10$ kA. In these runs the beam was observed to expand exponentially and the e-folding distance is determined from semilog plots of the change in the diagnostic beam radius; $R_{1/2}$, the radius which encloses one half of the beam current. The observed growth rates have been rescaled for a 10 kA, 1.0 cm beam by assuming the e-folding distance scales with the betatron wavelength. In Table III λ_β refers to the on-axis betatron wavelength, $\lambda_\beta = 2\pi R(I_A/2I_B)^{1/2}$. The magnitude of the growth rate is correctly predicted but the onset in f_m is observed to be $f_m = .6$ and not the predicted value of $f_m = .75$.

TABLE III

RINGFAST RUNS, BENNETT BEAM, BENNETT RETURN CURRENT

$\gamma = 100$
$R_B = .5$ cm
$R_P = .5$ cm

f_m varied by varying I_B, I_P

I_B Amps	I_P Amps	f_m	λ_{efold} cm	λ_β cm	Ω_I* cm^{-1}
100000.0	90000.0	.90	2.79	9.173	.056
10000.0	8000.0	.80	10.1	29.0	.049
50000.0	40000.0	.80	4.56	12.97	.049
40000.0	30000.0	.75	5.86	14.50	.042
30000.0	20000.0	.67	8.7	16.75	.033
25000.0	15000.0	.60	—	18.35	—

* Ω_I has been rescaled for a beam with $I_B = 10000.0$ A and $R_B = 1.0$ cm.

Conclusions

Stability boundary plots for the sausage mode show that even small fractional current neutralization can be destabilizing. The destabilizing effect of the return current is heightened if the return current is flowing within the beam current. Beam profiles with sharp edges are more unstable than those with smooth edges. For an on-axis return current a beam with $f_m > .5$ will not pinch. RINGFAST simulations confirm the existence of the $p = 0$ instability with $\eta^2 = 1.0$. The primary difference between RINGFAST and the theoretical analysis is that RINGFAST allows an arbitrary beam profile evolution while the theoretical analysis of reference 4 assumes a self-similar expansion. RINGFAST results do show somewhat larger regions of instability than predicted.

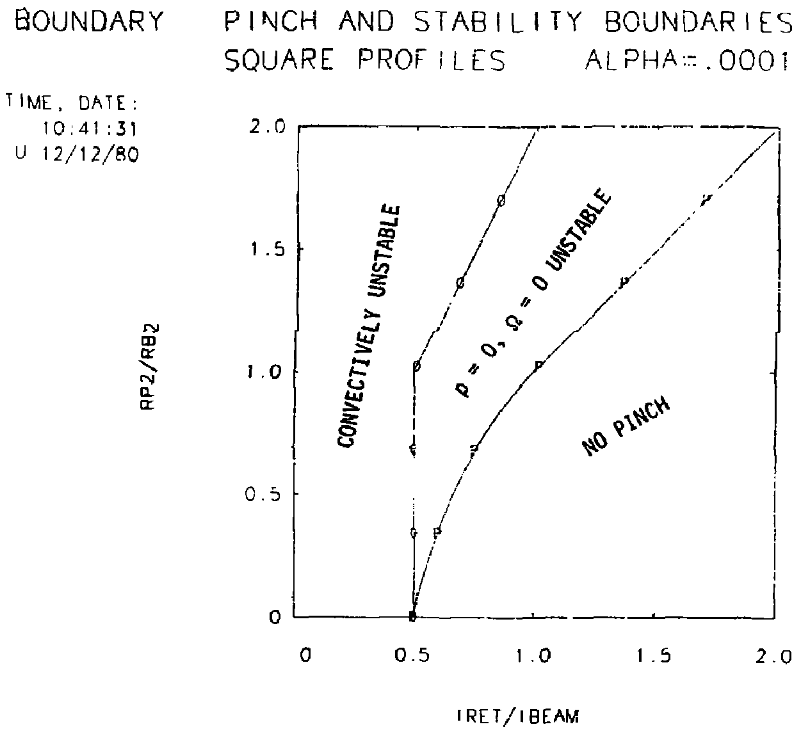

Figure 1. Stability boundaries in η^2 and f_m for a square beam with a square return current. For combinations of η^2 and f_m to the right of the boundary labelled "P" there is no pinch equilibrium. Between the boundaries labelled "P" and "O" the beam is unstable with $\Omega = 0$ and $p = 0$. Between the left hand side of the plot and the "O" boundary the beam is convectively unstable.

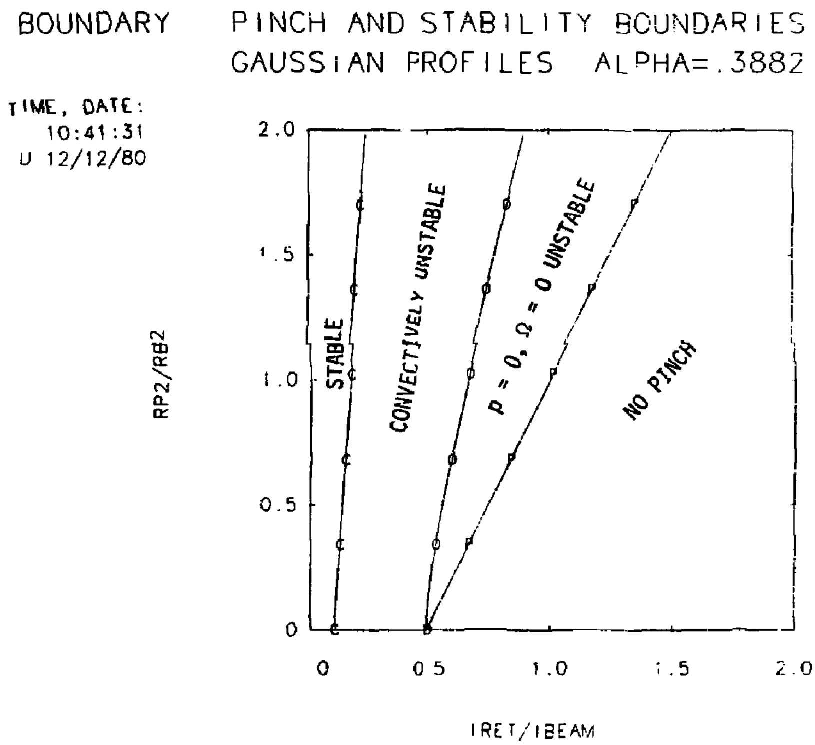

Figure 2. Stability boundaries in η^2 and f_m for a Gaussian beam with a Gaussian return current. For combinations of η^2 and f_m to the right of the boundary labelled "P" there is no pinch equilibrium. Between the boundaries labelled "P" and "O" the beam is unstable with $\Omega = 0$ and $p = 0$. Between "O" and "C' the beam is convectively unstable. For η^2 and f_m to the left of the "C" boundary the sausage mode is stable.

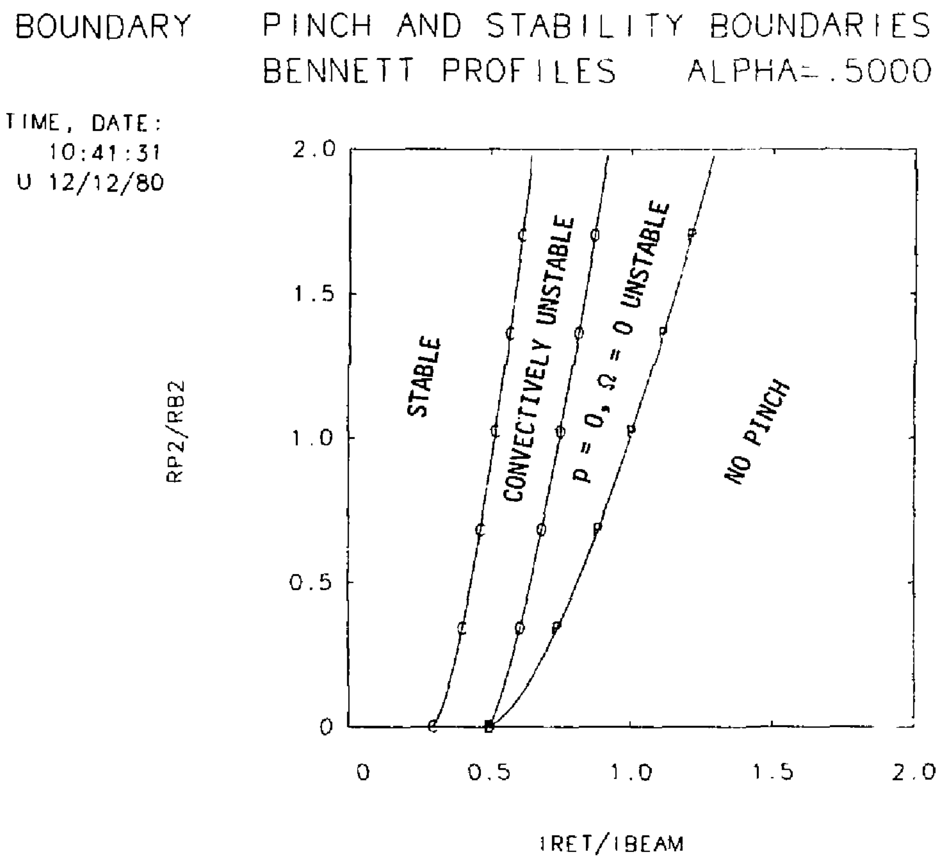

Figure 3. Stability boundaries in η^2 and f_m for a Bennett beam with a Bennett return current. For combinations of η^2 and f_m to the right of the boundary labelled "P" there is no pinch equilibrium. Between the boundaries labelled "P" and "0" the beam is unstable with $\Omega = 0$ and $p = 0$. Between "0" and "C" the beam is convectively unstable. For η^2 and f_m to the left of the "C" boundary the sausage mode is stable.

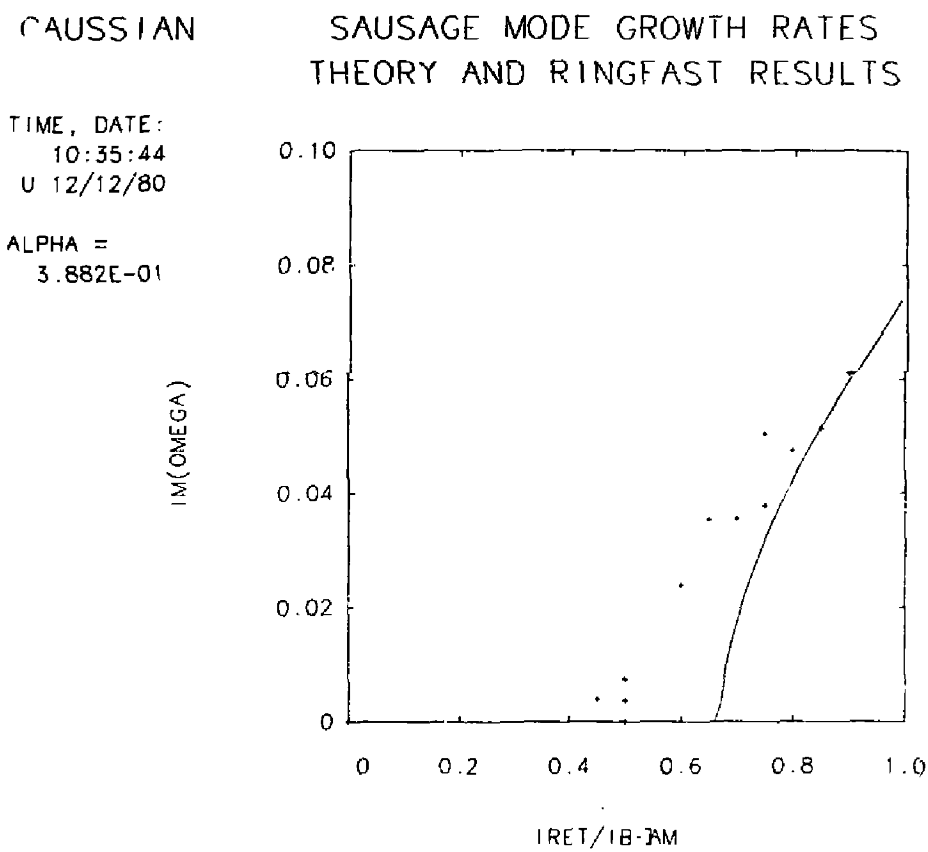

Figure 4. Theoretical and observed sausage mode growth rates versus f_m for a Gaussian beam with a Gaussian return current. The observed points are from RINGFAST runs delineated in Table II.

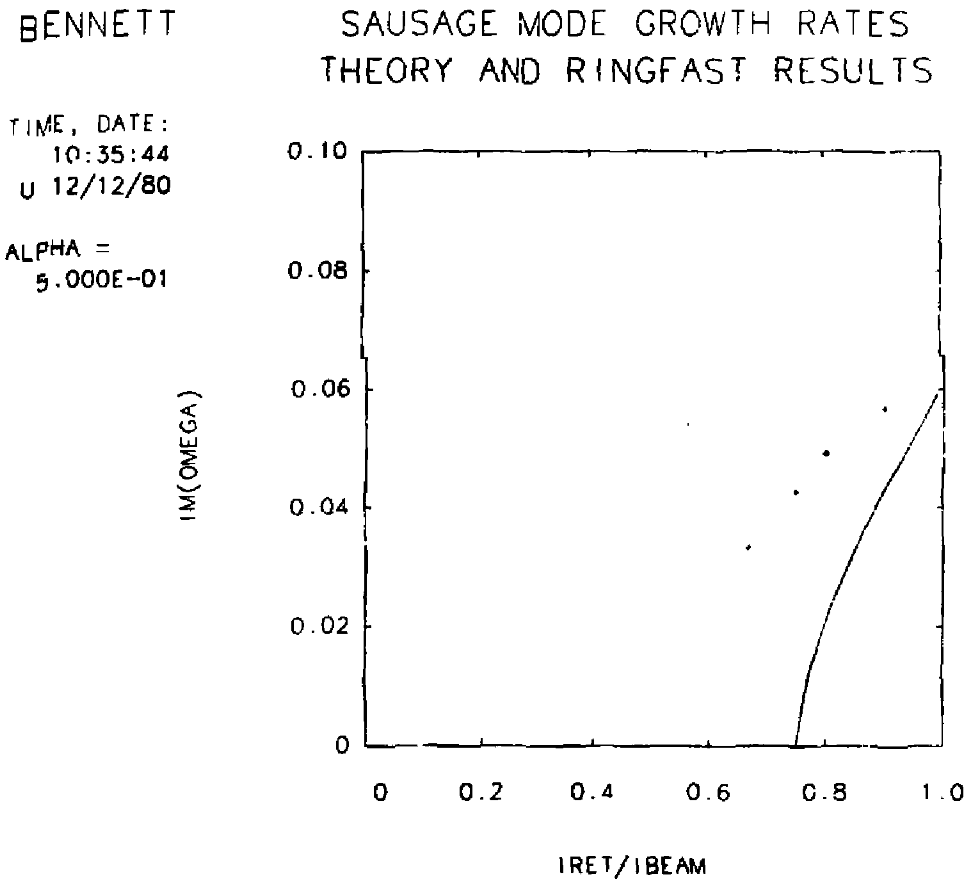

Figure 5. Theoretical and observed sausage mode growth rates versus f_m for a Bennett beam with a Bennett return current. The observed points are from RINGFAST runs delineated in Table III.

REFERENCES

1. F. W. Chambers Mathematical Models for the RINGBEARER Code, UCID-18302, Lawrence Livermore Laboratory, August 22, 1979.

2. F. W. Chambers RINGBEARER Results at 760 Torr, UCID-18609 Lawrence Livermore Laboratory (Report SNSI/Title U) March 15, 1980.

3. F. W. Chambers and J. A. Masamitsu Observations of Beam Sausaging Using the RINGBEARER Code, UCID - 18861, Lawrence Livermore Laboratory (Report SNSI/Title U) November 10, 1980.

4. E. P. Lee Sausage Mode of a Pinched Charged Particle Beam, UCIL - ?????, Lawrence Livermore Laboratory, August, [illegible].

5. H. S. Uhm and M. Lampe - to be published in Physics of Fluids.

6. E. P. Lee and S. S. Yu Model of Emittance Growth in a Self Pinched Beam UCID-18330 Lawrence Livermore Laboratory December 3, 1979.

7. F. W. Chambers Unstable Pulse Response in a Finite Beam Propagating a Finite Distance UCID-18301 Lawrence Livermore Laboratory September 20, 1979.

8. E. P. Lee Velocity Distribution in a Pinched Beam, UCID-18303 Lawrence Livermore Laboratory September 17, 1979.

VERSION RB8MEMO7

ENDTEXT